J Appl Electrochem (2007) 37:861–870
DOI 10.1007/s10800-007-9323-3

ORIGINAL PAPER

Oxidation kinetics of 4-methylanisole in methanol solution at carbon electrodes

Anis Attour · Sabine Rode · Tomas Bystron · Michael Matlosz · François Lapicque

Received: 31 May 2006 / Revised: 27 February 2007 / Accepted: 2 March 2007 / Published online: 28 March 2007

Abstract A quantitative investigation of the electrochemical oxidation of 4-methylanisole in methanol solution at carbon electrodes has been performed. The oxidation reaction is shown to be complex, resulting in the formation not only of the corresponding diacetal, but also of several intermediate products and side products. Voltammetric measurements and preparative batch syntheses reveal a substantial influence of the choice of both electrode material and supporting electrolyte. The highest selectivity and the most rapid reaction rates are observed at graphite electrodes with potassium fluoride supporting electrolyte, whereas polished surfaces of glassy carbon are far less reactive and result in substantial formation of side products. The observed oxidation kinetics can be represented with a simple empirical model, consisting of three oxidation steps in series yielding respectively an ether, an acetal and an ester. The experimental voltammetric curves have been used to determine the anisole diffusivity in the electrolyte solution and provide fitted values for the kinetic parameters of the three oxidation steps.

Keywords Anodic oxidation · 4-methylanisole · Carbon electrodes · Voltammetry · Batch cell · Selectivity

List of symbols

A	4-methoxy-toluene (or 4-methylanisole)
B	4-methoxy-benzylmethylether
b	Tafel parameter for the overall reaction (V^{-1})
b_j	Tafel parameter for the oxidation of species j (V^{-1})
C	4-methoxy-benzaldehyde-dimethylacetal
C_A	Reagent concentration (mol m^{-3})
C_{Ab}	Bulk concentration of reagent (mol m^{-3})
C_{js}	Surface concentration of product j (mol m^{-3})
D	4-methoxy-trimethoxytoluene
$\mathcal{D}$	Diffusion coefficient of the reacting species (m^2 s^{-1})
E	Electrode potential corrected for ohmic drop (V)
$E_{1/2}$	Half-wave potential (V)
F	Faraday constant (96487 C mol^{-1})
GC	Glassy carbon
I	Current (A)
i	Current density (A m^{-2})
i_j	Current density for the conversion of species j (A m^{-2})
i_k	Kinetically limited current density (A m^{-2})
i_{lim}	Mass-transfer limited current density (A m^{-2})
k	Rate constant for overall reaction (m s^{-1})
k_j	Rate constant for oxidation of species j (m s^{-1})
k'	Rate constant= $k\exp(-1.35b)$ (m s^{-1})
k_j'	Rate constant= $k_j\exp(-1.35b_j)$ (m s^{-1})
k_m	Mass-transfer coefficient (m s^{-1})
m	Tafel slope (mV/dec)
n_e	Number of electrons transferred in the reaction per mole of reagent
n_{eff}	Number of electrons effectively consumed per converted reagent
n_{int}	Cumulative number of electrons exchanged
Q	Electrical charge (C)
Q_{max}	Theoretical charge required for total conversion of reagent (C)
R	Ideal gas constant (8.314 J mol^{-1} K^{-1})

A. Attour · S. Rode · M. Matlosz · F. Lapicque (✉)
Laboratoire des Sciences du Génie Chimique, CNRS-ENSIC, BP 20451, Nancy Cedex 54001, France
e-mail: lapicque@ensic.inpl-nancy.fr

T. Bystron
Institute of Chemical Technology Prague, Technicka 5, Prague 16628, Czech Republic

T Cell temperature (K)
V_R Cell volume (m^3)

Greek letters

α Charge transfer coefficient
v Kinematic viscosity of the solution ($m^2\ s^{-1}$)
v_{ej} Number of electrons involved in the rate-determining step of product j oxidation
ω Angular rotation rate (s^{-1})

1 Introduction and objectives

The anodic oxidation of toluenes to aryl aldehydes has been the subject of numerous investigations since the initial studies in the late 1950s by Venkatachalapathy et al. [1]. More recent studies have been published by Wendt et al. [2–4] and by Kramer et al. [5], and a summary of the principal characteristics of aryl aldehyde electrosynthesis can be found in [6]. Industrial interest in the synthesis is mainly due to the widespread use of functionalised aldehydes in fine chemistry.

The electrochemical synthesis is generally performed on carbon electrode materials. In contrast to toluene, the presence of the methoxy group (OCH_3) in ring position 4 (such as in 4-methylanisole) activates the substrate methyl group, thereby allowing its direct oxidation. Furthermore, the presence of the methoxy group deactivates the benzene ring, thus avoiding side reactions due to ring cleavage [4].

In methanol solutions, the overall reaction can be described as follows [3, 4]:

$$ArCH_3 + MeOH - 2e \rightarrow ArCH_2OMe + 2H^+$$
(Ether formation)

$$ArCH_2OMe + MeOH - 2e \rightarrow ArCH(OMe)_2 + 2H^+$$
(Diacetal formation)

$$ArCH(OMe)_2 + H_2O \xrightarrow{H^+} ArCHO + 2MeOH$$
(Diacetal hydrolysis to aldehyde)

$$ArCH(OMe)_2 + MeOH - 2e \rightarrow ArC(OMe)_3 + 2H^+$$
(Ester formation)

where Ar denotes the aryl part of the molecule, 4-methoxy-toluene for the case investigated in the present study. On carbon electrodes, the first two electrode reactions have been shown to be sequences of electron transfer and chemical deprotonation of rearrangements as suggested by Wendt and Bitterlich [3] and recently by Lindermeier [7]:

$$ArCH_3 \xrightarrow{-e} Ar\text{-}CH_3]^{\cdot+} \xrightarrow{-H^+} Ar\text{-}CH_2]^{\cdot} \xrightarrow{-e} Ar\text{-}CH_2]^{+} \xrightarrow{-H^+,+MeOH} ArCH_2 - OMe$$

with the side reaction

$$2Ar\text{-}CH_3^+ \rightarrow (Ar\text{-}CH_3)_2^{2+} \rightarrow \text{oligomers}$$

The side reaction is favoured in acidic solvents such as acetonitrile as recently shown by Haj Said et al. [8]. Conversely, the addition of alkaline substances such as lutidine, as suggested by Wendt et al. [4], favour the first deprotonation step. Deprotonation has been shown to be accelerated by heterogeneous catalysts such as graphite, and it is generally established that the second electron transfer leading to $Ar–CH_2^+$ requires a substantially lower anodic potential than that of the first deprotonation [9]. It would be expected, therefore, that the oxidation of 4-methoxytoluene to the corresponding ether should proceed as a rapid two-electron transfer. Considering a charge-transfer coefficient α of 0.5, this would correspond to a Tafel slope of 59.1 mV/decade at 25 °C, in agreement with the experimental observations of Wendt and Bitterlich [3]. The oxidation of 4-methoxybenzyl methyl ether has been reported by the same authors as a rapid process with a more rapid deprotonation and comparable values of charge-transfer rate. The oxidation of the diacetal occurs at a potential 200 mV more positive than that of anisole. Graphite electrodes exhibit higher reactivity for the first deprotonation step: for the case of 4-methylanisole, this results in half-wave potentials 65 mV less positive on graphite than on glassy carbon and platinum [3].

Preparative batch oxidations of various toluenes have been carried out in traditional electrochemical cells by Wendt et al. [4, 10], and recently batch syntheses in ultrasonic devices have also been performed [7]. For the case of 4-methylanisole, the number of electrons consumed in the conversion has been observed to increase with time in the batch syntheses from 2.5 in the early stages of reaction to 4 in the later stages, suggesting formation of an ether intermediate in the initial stages of oxidation [4]. Use of potassium fluoride as a supporting electrolyte resultes in higher diacetal yields than with other salts.

In recent years, a number of new electrochemical devices, including thin-gap cells [11, 12] and segmented electrodes [13] have been proposed to improve the performance of the anodic oxidation of toluenes to aryl aldehydes, with particular interest focused on the electrochemical oxidation of 4-methylanisole, performed

industrially for the production of anisaldehyde [6, 14, 15]. In order to pursue investigation of the performance characteristics of these new devices, more quantitative kinetic information for the anodic oxidation reactions is required.

The objective of the present work is therefore to investigate further the reaction mechanism of the anodic oxidation of toluenes by completing the existing experimental studies in the literature with a more quantitative examination of the variation in electro-oxidation kinetics as a function of electrode material and supporting electrolyte. For this purpose, voltammetric measurements at rotating disk electrodes (RDE) are employed, and the experimental results fitted to a simplified empirical kinetic model involving a series of 2-electron transfer processes for the overall oxidation. Additional preparative batch syntheses are used to provide further qualitative support for the proposed mechanistic approach. The final quantitative kinetic expressions, based on the fitted kinetic parameters, are intended to be used in subsequent work to evaluate the potential interest of novel electrochemical reactor designs.

2 Experimental section

2.1 Chemicals and materials

The reactant, 4-methylanisole of purissimum grade, was purchased from Acros Organics. Methanol, purchased from Merck, was of HPLC grade. Supporting electrolytes, namely sodium perchlorate at 0.4 or 0.8 M, lithium perchlorate at 0.8 M, and potassium fluoride at 0.1 or 0.2 M, were of analytical grade and purchased from Acros Organics. The viscosity of the solutions was measured using an Ubbelohde capillary tube with laminar flow of the solution: kinematic viscosity ν varied from 0.7×10^{-6} m^2 s^{-1} for 0.2 M KF to 0.85×10^{-6} m^2 s^{-1} for 0.8 M perchlorate solutions.

For the sake of simplicity, the various compounds involved in the synthesis are denoted anisole, ether and acetal: the presence of aldehyde formed from acetal by hydrolysis is accounted for in the acetal mole number. Analysis of the fractions collected in the batch experiments was carried out by HPLC (Shimadzu) using an Inertsil ODS-3 250×4.6 mm column with an internal diameter of 5 μm and with a 55:45 acetonitrile–water eluent. The various compounds were detected at 230 nm.

2.2 Electrode materials

Glassy carbons (Sigradur) were purchased from HTW-Hochtemperatur Werkstoff, Germany, and graphite materials from Goodfellow. The rotating disk electrodes (RDE) used were constructed from a PTFE shaft with a stainless steel connection, and a 3.0 mm cylindrical sample of carbon electrode material to be investigated. In addition to the graphite disk electrode, two RDE were machined with glassy carbon (GC) as follows:

1. A small GC disk, 1 mm thick, was pasted on top of the stainless steel support. The conducting paste also allowed the small gap between the cylinder surface and the machined PTFE piece to be filled. Because of its shiny appearance, this surface will be called ''polished''.
2. A one centimetre GC cylinder from HTW was inserted into the PTFE-stainless steel shaft. The length of the cylinder allowed perfect alignment of the two surfaces. The active surface appeared far less shiny and has been called ''cut'', because the cylinders were produced by cutting without further polishing of the small surface of the disk.

2.3 Electrochemical cells

RDE investigations were carried out using a 150 cm^3 glass cell, provided with a glass cover. The counter electrode was a 50 cm^2 sheet of expanded platinised titanium. The reference electrode was a saturated calomel electrode (SCE, 0.242 V/NHE).

Batch runs were made in a 400 mL glass reactor at ambient temperature, with 200 mL of 10 mol m^{-3} anisole solutions at the start. The working electrode was a 5×5 cm^2 carbon sheet (''polished'' GC or graphite) with an immersed surface of approximately 40 cm^2 corresponding to both sides of the immersed carbon sheet. A 120 cm^2 sheet of expanded platinised titanium acted as the counter electrode; the cell was provided with a SCE reference electrode and magnetic stirring.

All experiments were performed with a potensiostat (PGSTAT 10 from Autolab).

3 Voltammetric investigations

3.1 Experiments and interpretation of the first anodic wave

Voltammetric studies were conducted at low scan rate (3 mV s^{-1}) on RDE of various electrode materials. The disk electrode was rotated at 100, 400 or 900 rpm, and the anisole concentration was 2.5, 5 or 10 mol m^{-3}. Voltammetric curves were corrected for ohmic drop by using the cell resistance previously measured by impedance spectroscopy. The residual current measured without anisole

was then subtracted. The values of electric current recorded control measurements at fixed potential were in agreement with the currents measured in the voltammetric tests, with deviations less than 15%.

Typical voltammetric curves recorded in 0.8 M $NaClO_4$ are shown in Fig. 1. For all cases the voltammograms exhibited a well-defined oxidation wave attributed to formation of acetal. A second oxidation wave appeared at more positive potentials: the resolution of the second wave from the overall curve depended on the RDE materials. The half-wave potential of the first oxidation was observed near 1.35 V/SCE at graphite surfaces, and near 1.42 V/SCE for the GC surfaces: these potential values are nearly 200 mV more positive than those reported in [3]. The deviations could be due to the different origins of the carbon materials used. Well-defined plateaus were obtained with graphite and polished GC. The second current wave appeared at 1.50 V on graphite and at 1.65 V for the GC surfaces: the current increased more regularly on the cut GC surface, whereas the plateau was better defined with the polished GC electrode. The second wave has been attributed to acetal oxidation, as shown in previous works [3]; however the accuracy in this part of the *i–E* curves was poor due to the significant contribution of the residual current to the overall current. In addition, electrode side reactions between the solvent and intermediate species are likely [4].

Initial interpretation of the curves was focused on estimation of kinetic parameters related to the first oxidation wave. The data were analysed using the Koutechky–Levich equation for the current density under mixed-control (kinetic and mass transfer) [16]:

$$\frac{1}{i} = \frac{1}{i_k} + \frac{1}{i_{\lim}} = \frac{1}{n_e F k' C_A \exp(bE)} + \frac{1}{0.621 n_e F C_A \mathcal{D}^{2/3} \omega^{1/2} \nu^{-1/6}} \quad (1)$$

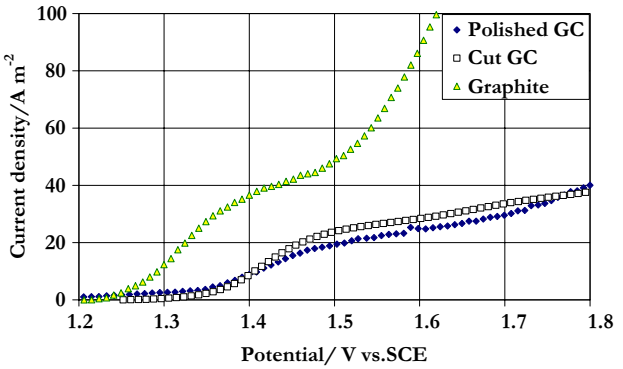

Fig. 1 Voltammetric oxidation curves of 4-methylanisole (5 mol m^{-3}) at a carbon RDE in 0.8 M $NaClO_4$ methanol solution; rotation rate = 100 rpm; influence of the carbon electrode material

For the overall oxidation to acetal, $n_e = 4$, and the electrode rate constant k' is defined at 0V/SCE. For convenience, modified electrode rate constant, k, was introduced in Eq. 1 with an arbitrary potential shift of 1.35 V/SCE into a potential zone for which effective oxidation occurs:

$$k' = k \exp(-1.35b) \quad (2)$$

The current density is than expressed as follows:

$$\frac{1}{i} = \frac{1}{n_e F C_A k \exp[b(E - 1.35)]} + \frac{1}{0.621 n_e F C_A \mathcal{D}^{2/3} \omega^{1/2} \nu^{-1/6}} \quad (3)$$

For each concentration of 4-methylanisole, C_A, the data recorded at the various rotation rates were fitted to Eq. 3. As shown in Fig. 2, the overall model allows representation only of the first anodic wave related to acetal formation, i.e., for potentials below 1.6 V/SCE for glassy carbon, as further oxidation phenomena were not accounted for.

Values for k were typically of the order of 10^{-6}–10^{-5} m s^{-1}, with higher values with graphite surfaces (Table 1). The Tafel slope, m, can be expressed in terms of Tafel parameter, b, as follows:

$$m = \frac{2303}{b} (\text{mV/dec}) \quad (4)$$

Tafel slopes were approximately 139 mV/decade on polished GC surfaces, 69 mV/decade on graphite and 74 mV/decade on freshly-cut GC surfaces (Table 1). This result, observed with all of the supporting electrolytes studied (sodium and lithium perchlorates, potassium fluoride), partly contradicts Wendt's conclusions [3] according to which the oxidations of toluene and ether are very fast

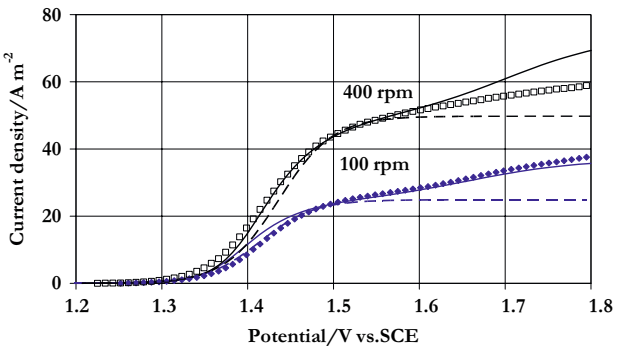

Fig. 2 Voltammetric oxidation curves of 4-methylanisole (5 mol m^{-3}) at a cut GC surface in 0.8 M $NaClO_4$ methanol solution; comparison of experimental data to fitted model: dotted lines are for the model limited to the first anodic wave (Eq. 3) and solid lines for the fitted model including consecutive oxidation reactions

Table 1 Results of the overall interpretation of the voltammetric curves

Electrode	Salt	C_A	$\mathcal{D}$	k	m
Cut GC	LiClO4	5	6.4	2	76
Cut GC	NaClO4	2.5	5.4	5.5	71
		5	5.1	1.6	72
		10	6.7	4.9	74
Graphite	NaClO4	5	9.8	36	69
Polished GC	LiClO4	5	4.4	1.1	101
Polished GC	NaClO4	2.5	5.1	5.9	159.5
		5	5.4	3.6	139
		10	6.5	4.6	171
Polished GC	KF	5	4.2	2.9	139
		10	4	4	150

Anisole concentration C_A in mol m^{-3}, $\mathcal{D}$ in 10^{-10} m^2 s^{-1}, k in 10^{-6} m s^{-1}, and m in mV/decade. Supporting electrolyte (salt) concentrations of $NaClO_4$ and $LiClO_4$: 0.8 M, KF: 0.2 M

two-electron oxidations with an overall Tafel slope of the 4-electron reaction of approximately 60 mV/decade.

The diffusion coefficient $\mathcal{D}$ of 4-methylanisole was found to vary from 4 to 6.7×10^{-10} m^2 s^{-1} depending on the electrolyte used, with the exception of the graphite electrode for which a higher value of the diffusivity was obtained (Table 1). The difference is likely due to the roughness of the graphite surface.

3.2 Model for consecutive anodic waves

In order to present polarization behaviour beyond the first anodic wave, the voltammetric curves were interpreted by considering three oxidations in series, yielding ether, acetal and ester-products B, C, and D respectively:

$$A - 2e \rightarrow B \tag{5a}$$

$$B - 2e \rightarrow C \tag{5b}$$

$$C - 2e \rightarrow D \tag{5c}$$

The model was developed on the basis of the following assumptions:

1. The three reactions are assumed to be irreversible. Each reaction involves two electrons and corresponds to consumption of species (j), j = A, B or C.
2. No adsorption phenomena are considered.
3. The area of the RDE is small enough in comparison with the volume of the electrolyte solutions, that the bulk concentrations of species B, C, and D can be neglected.
4. The model is written at steady-state, in both the bulk and at the electrode surface.

The following Tafel laws were considered:

$$i_j = n_e F k'_j C_{js} \exp(b_j E) \quad \text{with} \quad j = \text{A, B or C} \tag{6}$$

where n_e is the number of electrons involved, n_e = 2, and C_{jS} the surface concentration of species j. Parameters k'_j and b_j are the kinetic parameters of the oxidation of species j. The partial control of processes by diffusion-convection results in depletion of the reactive species near the electrode surface: A diffuses toward the electrode, with a mass transfer coefficient k_m depending on both its diffusivity and the local hydrodynamics. The current density of the first oxidation can therefore be written as follows:

$$i_A = n_e F k_m (C_{A_b} - C_{A_s}) \tag{7}$$

The surface concentration can then be deduced as a function of the bulk concentration C_{Ab} and the potential E:

$$C_{A_s} = \frac{k_m C_{A_b}}{k_m + k'_A \exp(b_A E)} \tag{8}$$

Mass balances on species B and C can be written by equating their production flux to their consumption flux, plus the flux transferred from the electrode surface, as follows:

$$n_e F k'_A C_{A_S} \exp(b_A E) = n_e F k'_B C_{B_S} \exp(b_B E) + n_e F k_m C_{B_S} \tag{9a}$$

$$n_e F k'_B C_{B_S} \exp(b_B E) = n_e F k'_C C_{C_S} \exp(b_C E) + n_e F k_m C_{C_S} \tag{9b}$$

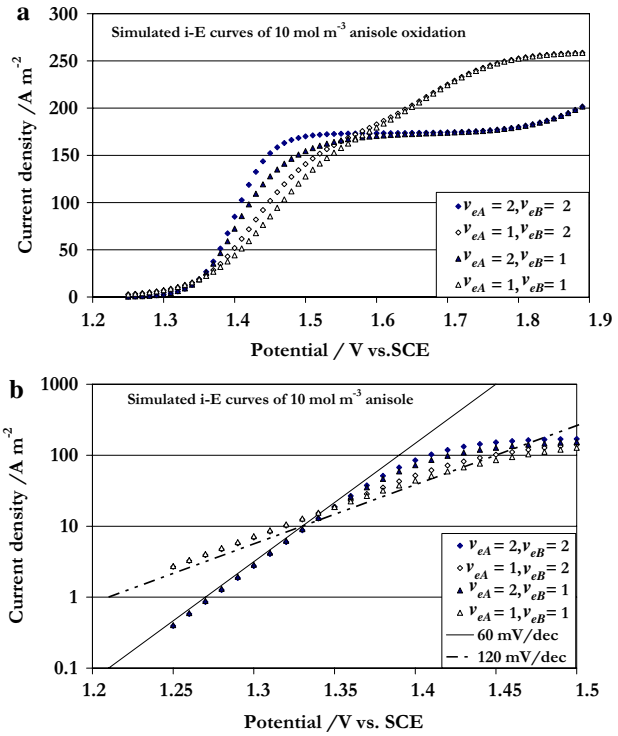

Fig. 3 Simulated voltammetric curves for 10 mol m^{-3} anisole concentration as a function of the values for number of electrons involved in the rate-determining step v_{eA} and v_{eB}. The values of the other parameters are provided in the text. (**a**) Upper figure: linear plot; (**b**) lower figure: Tafel plot

The balance expressions (9) lead to the following expressions for the surface concentrations C_{B_S} and C_{C_S}:

$$C_{B_S} = C_{A_S} \frac{k'_A \exp(b_A E)}{k_m + k'_B \exp(b_B E)} \tag{10a}$$

$$C_{C_s} = C_{B_S} \frac{k'_B \exp(b_B E)}{k_m + k'_C \exp(b_C E)} \tag{10b}$$

Concentrations C_{B_S} and C_{C_S} are calculated from the surface concentration C_{A_S} and potential E, taking into account rate constant k'_j, Tafel parameter b_j, and mass transfer coefficient k_m. The overall current density for the electrochemical reaction is the sum of contributions i_j:

$$i = i_A + i_B + i_C \tag{11}$$

The mass transfer coefficient k_m was calculated using the Levich equation:

$$k_m = 0.621 \mathcal{D}^{2/3} \omega^{1/2} \nu^{-1/6} \tag{12}$$

For the sake of simplicity, and in spite of the noticeable difference in size of species A, B and C, the diffusion coefficient of all species has been assumed to be the same, and will be denoted D in the text. Finally, as for the model of the first anodic wave, we operated a potential shift by considering kinetic constants k'_j defined as:

$$k'_j = k_j \exp(-1.35 b_j) \tag{13}$$

3.3 Simulation of the (i–E) curves

The model described above involves seven parameters whose determination from experimental data can be difficult. The sensitivity of the model, in particular to the values of parameters b_j was examined. For this purpose, the charge transfer coefficient α was fixed at 0.5. The number of electrons involved in the rate-determining step, v_{ej}, was chosen to be 1 or 2. The Tafel parameter b_j was deduced from the v_{ej} values as follows:

$$b_j = \frac{\alpha v_{ej} F}{RT} \tag{14}$$

where R denotes the ideal gas constant (8.314 J mol^{-1} K^{-1}) and T the absolute temperature (298 K). Depending on v_{ej}, b_j varies from 19.46 to 38.92 V^{-1}, respectively, corresponding to Tafel slopes from 118.2 to 59.1 mV/decade.

Simulations have been made by varying v_{eA} and v_{eB} between 1 and 2, which represents four combinations, for a reagent concentration of 0.01 M anisole. The oxidation plateau of acetal calculated for $v_{eC} = 2$ usually appeared far better defined than the experimental (*i–E*) variations: for this reason, coefficient v_{eC} was fixed at 1 in the preliminary simulations. The diffusion coefficient $\mathcal{D}$ was taken to be 10^{-9} m^2 s^{-1}, constants k_A and k_B were taken to be 10^{-5} m s^{-1} for $E = 1.35$ V/SCE, whereas constant k_C was assumed to be related to k_A by $k_A \exp(-0.25 b_A)$, corresponding to an assumed 250 mV shift between the two waves. The simulation results reported in Fig. 3 show the effect of (v_{eA}, v_{eB}) values on the profiles of (*i–E*) curves. Separate estimation of coefficients v_{eA} and v_{eB} by fitting experimental (*i–E*) curves was shown to be possible. Moreover the average Tafel slope of the first wave was near 60 mV/decade when $v_{eA} = 2$, and 120 mV/decade when $v_{eA} = 1$, regardless of v_{eB}.

3.4 Application of the model to experimental voltammetric curves

The model was fitted to experimental data by least-square minimisation on the deviations of the current density, using the gradient method available with Excel™ software (Microsoft). Preliminary tests revealed that the (*i–E*) curves

could not be perfectly fitted with integer values for v_{eC}. Coefficients v_{eA} and v_{eB} were varied as integers in the fitting, whereas parameters k_j and v_{eC} were varied without any restriction. Table 2 summarises the values of the fitted parameters for all conditions tested. Tafel plots of theoretical and experimental (i–E) variations exhibited a slight discrepancy, corresponding to the fact that the overall Tafel slope, related to the product (αv_{eC}), was slightly larger then the expected values given above: the actual charge transfer coefficient involved in the first two steps likely differs slightly from the postulated value of 0.5. However, as exemplified in Fig. 2, the agreement allowed by this model was far better than the overall interpretation, in particular because acetal oxidation was accounted for. In agreement with the preliminary observations made above, coefficient v_{eA} could be taken to be 2 with cut glassy carbon, whereas v_{eB} was equal to 1. Polished glassy carbon surfaces were probably deactivated by the polishing procedure and v_{eA} was found to be 1. The faster oxidation to ether observed on graphite with the same electron number for the second step (v_{eB}) should result in more significant accumulation of ether in the solution: this was actually observed (Fig. 8) as discussed in the following section. Better agreement was found in most cases for $v_{eC} = 0.8$, except for graphite for which v_{eC} was taken to be 1: in fact the numerical result means that the product (αv_{eC}) is equal to 0.4 for the two GC materials.

Rate constants k_A and k_B could be estimated within 15%. The two constants are of the same order of magnitude with the overall constant k, in the range 10^{-6}–10^{-5} m s^{-1} (Table 2). However, contrary to Wendt's conclusions [3], k_B was generally slightly smaller than k_A, except for graphite, for which the two rate constants differ more significantly. Constant k_C was estimated with poor accuracy because of the significant current due to side reactions: in addition to the residual current, methanol may be involved in the oxidation of aryl compounds. Therefore, subtraction of the residual current over 1.7 V (for ohmic correction) distorts the (i–E) curves in this potential domain. The constant k_C could thus only be estimated to a factor of two.

The diffusion coefficient $\mathcal{D}$ was estimated from each series of (i–E) curves within 8%, and the values obtained were very close to those found with the overall model (Tables 1 and 2). The experimental values of diffusivity were compared to theoretical estimates from published correlations. The correlations proposed by Tyn and Calus [17] and Siddiqi and Lukas [18] were selected for the comparison since they were established for organic molecules dissolved in solvents of a low dielectric constant, such as methanol. Application of the correlations to the present case yielded $\mathcal{D}$ estimates at 1.37 and 1.31×10^{-9} m^2 s^{-1} respectively. These values are significantly higher than the experimental diffusion coefficients listed in Table 2. The noticeable deviation between theory and experiment could partly be due to the presence of supporting electrolyte in the solvent but also due to electrode surface deactivation.

It was observed that the concentration of 4-methylanisole had no significant effect on the values of the kinetic and diffusion parameters. A more significant influence of the supporting electrolyte and electrode material was observed. In particular, graphite exhibits a far larger activity in the three oxidation steps, with rate constants 3–30 times larger than at glassy carbon (Tables 1, 2).

Table 2 Values of the kinetic parameters deduced from fitting of the experimental data to the empirical model

Electrode	Salt	C_A	$\mathcal{D}$	k_A	k_B	k_C	v_{eA}	v_{eB}	v_{eC}
Cut GC	$LiClO_4$	5	6.9	4	2	0.01	2	1	0.8
Cut GC	$NaClO_4$	2.5	5.8	9	6	0.1	2	1	0.8
		5	4.8	3	5	0.1	2	1	0.8
		10	7	10	6	0.1	2	1	0.8
Graphite	$NaClO_4$	5	10	100	20	1	2	1	1
Polished GC	$LiClO_4$	5	4.5	3	3.5	0.01	1	1	0.8
		2.5	4	8	7	0.01	1	1	0.8
Polished GC	$NaClO_4$	5	5	6	4	0.01	1	1	0.8
		10	5.5	6	4	0.01	1	1	0.8
Polished GC	KF	5	4	4.5	2	0.01	1	1	0.8
		10	4	4	3	0.01	0.8	0.9	0.8

Anisole concentration C_A in mol m^{-3}, $\mathcal{D}$ in 10^{-10} m^2 s^{-1}, k_j in 10^{-6} m s^{-1}. The charge transfer coefficient α was fixed at 0.5. Supporting electrolyte (salt) concentrations of $NaClO_4$ and $LiClO_4$: 0.8 M, KF: 0.2 M

4 Batch oxidation of 4-methylanisole

The applied current was fixed at 75 mA, corresponding to approximately 2 mA cm^{-2}, so that the electrode potential in the early stages was in the potential domain of the first oxidation wave. The potential was continuously monitored for the 150 min duration of each run. One-millilitre samples were taken every 15 min for analysis. The changes in volume and in the mole amount of anisole induced by sampling were accounted for in the calculations. The electrical charge passed, Q, was normalized with respect to the theoretical charge, Q_{max}, required for total conversion of the reagent to acetal. No run was allowed to continue beyond $Q/Q_{max} = 1$. All runs were duplicated and a third test was carried out if too large a discrepancy was observed between the first two runs. The results shown here are the averages obtained.

The anisole conversion was not substantially affected by the nature of the supporting electrolyte (Fig. 4), but faster conversion was observed with glassy carbon than with graphite. The dimensionless plot used suggests that the current efficiency calculated on the basis of 4 electrons exchanged was larger than unity, in particular for the GC surface: the electrochemistry of anisole oxidation to acetal cannot be modelled perfectly by a simple 4-electron process to acetal. The concentration of acetal normalised by the initial anisole concentration (i.e., the acetal yield) was plotted versus Q/Q_{max} and is shown in Fig. 5. For graphite, acetal accumulated regularly in the liquid for any of the two electrolytes used and for Q/Q_{max} up to 0.7 before levelling off: the dimensionless concentration attained 50 % after complete consumption of anisole. With glassy carbon, the supporting electrolyte exerted a strong effect: the acetal concentration remained nearly constant at 0.45 with KF for Q/Q_{max} larger than 0.60, whereas it exhibited a flat maximum with sodium perchlorate for Q/Q_{max} near

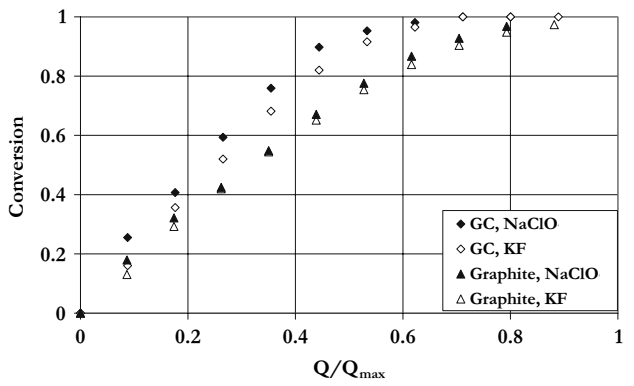

Fig. 4 Conversion of anisole (10 mol m^{-3}) versus the dimensionless charge. Influence of the carbon electrode material (polished glassy carbon or graphite) and nature of supporting electrolyte

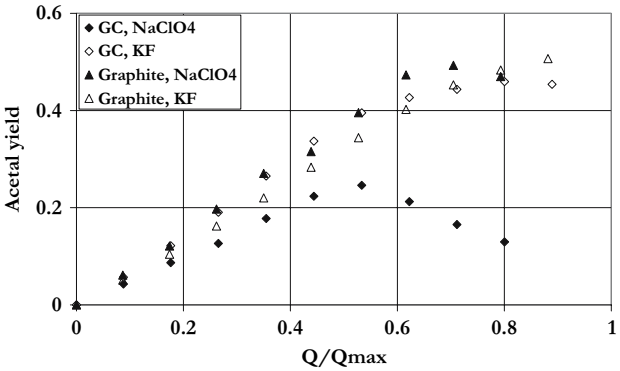

Fig. 5 Acetal yield (including aldehyde formation) versus the dimensionless charge. Influence of the carbon material (polished glassy carbon or graphite) and nature of supporting electrolyte

50%, corresponding to significant acetal oxidation in the second half of the run. Although far less visible, the side oxidation of acetal was also observed on the graphite electrode (Fig. 5). The highest yields of acetal were obtained with potassium fluoride, which was selected for further oxidation experiments.

The electrode potential was shown to increase regularly during a run (Fig. 6), due to the steady consumption of anisole. For the graphite surface (Fig. 6a), the effect of the electrolyte although moderate is visible: with a KF

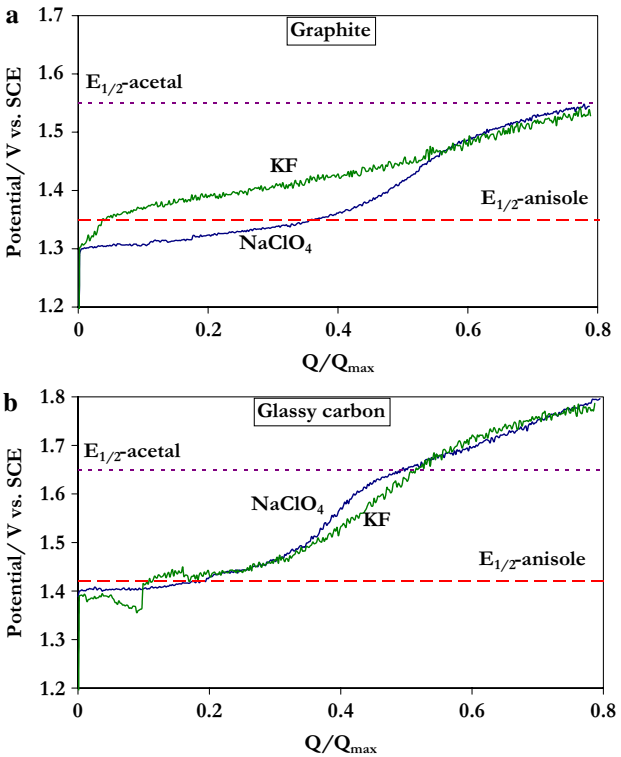

Fig. 6 Variation of the graphite potential during a batch run. (**a**) upper figure: graphite; (**b**) lower figure: glassy carbon

electrolyte, the potential at the end of a run was below the half-wave value of the second oxidation, which corresponds to moderate acetal oxidation in the final part of the run (Fig. 5). With sodium perchlorate, the higher potential value (Fig. 6a) corresponds to more effective consumption of acetal. For glassy carbon (Fig. 6b), the potential measured with $NaClO_4$ is higher than the half-wave potential of acetal oxidation ($E_{1/2}$ -acetal) from $Q/Q_{max} = 0.5$, which explains the noticeable acetal consumption mentioned above. With KF, although the potential variation was similar to that with $NaClO_4$, the consumption of acetal was less significant (Fig. 5).

The number of electrons effectively consumed per converted anisole molecule, n_{eff}, was calculated from the slope of anisole concentration C_A versus time:

$$\frac{1}{n_{\text{eff}}} = -\frac{dC_A}{dt}\frac{V_R F}{I} \approx -\frac{\Delta C_A}{\Delta t}\frac{V_R F}{I} \qquad (15)$$

where ΔC_A is the concentration variation within period Δt, V_R is the solution volume and I the applied current.

At the beginning of the reaction, n_{eff} was approximately 2.5 for graphite and 2.1 for the polished GC electrode: these values are in good agreement with previous data [4], confirming that acetal is not a primary product of the oxidation. The cumulative (integral) number of electrons exchanged, n_{int}, was also calculated by integrating n_{eff} between $t = 0$ and t. The coefficient n_{int} was nearly constant during the first part of the run and increased regularly from $Q/Q_{max} = 0.5$ (Fig. 7). Oxidation of anisole consumes less than four electrons at the beginning of the batch experiment, indicating that a substantial part of the anisole is initially oxidized to benzyl ether or to other products of lower oxidation state than acetal.

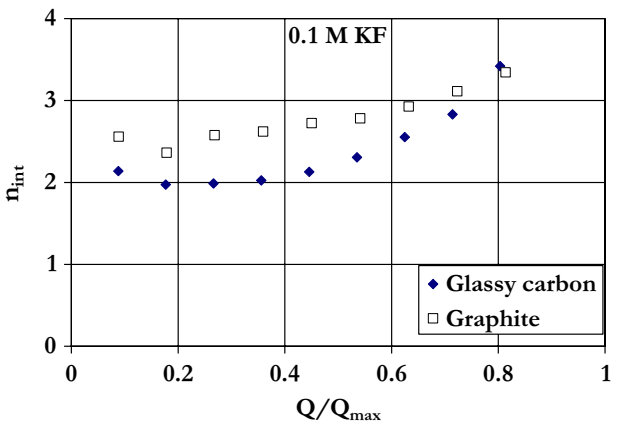

Fig. 7 Cumulative number of electrons consumed per anisole molecule in KF-methanol solutions versus the normalized electrical charge

In addition to anisole, ether, acetal and aldehyde, HPLC analysis revealed the existence of other products. Some of these could be identified by mass spectroscopy: ester, dimers at percent levels, but also side-products formed by addition of methanol to the benzene ring, as reported in [4]. The sum of these products is referred to as ''secondary products''. The variation of the chemical composition of the KF-methanol solution during the run is shown in Fig. 8. As expected, ether appeared as an intermediate compound and its concentration exhibited a flat maximum for Q/Q_{max} around 0.3–0.4. Significant amounts of ether were obtained with graphite, in comparison with GC: this is consistent with the values for constants k_A and k_B, since the high (k_A/k_B) ratio determined for the graphite anode (Table 2) should result in significant accumulation of ether in the cell. The variations of acetal and anisole concentrations have been discussed above. The formation rate of secondary products and their nature seems to depend significantly on the electrode material: on the graphite surface (Fig. 8a), secondary products were regularly formed during a run and consisted of both dimers produced from the first intermediate cation, and more oxygenated species such as esters. On GC surfaces (Fig. 8b), the secondary products were formed rapidly in the first part of the oxidation run. Consistent with the low value for n_{eff}, this observation

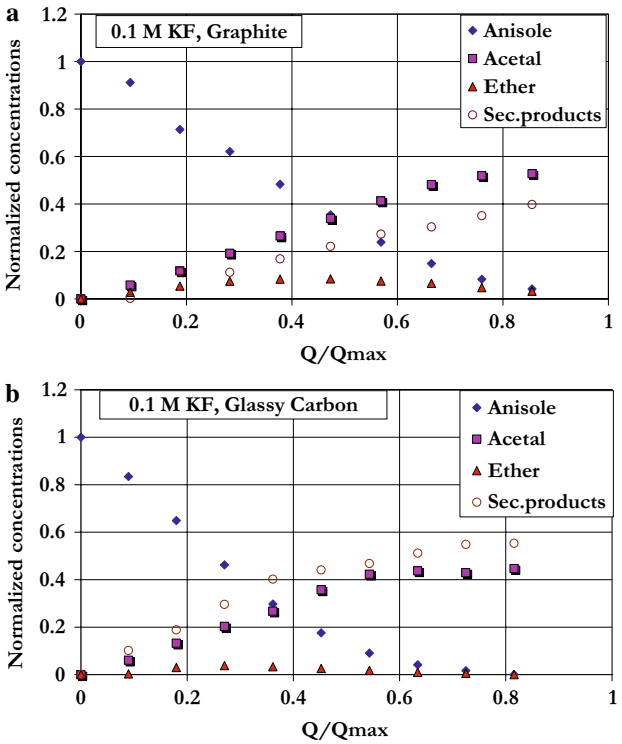

Fig. 8 Composition of the solution during a batch run. Influence of the electrode material. (**a**) upper figure: graphite; (**b**) lower figure: polished glassy carbon

would mean that the contribution of dimers—or slightly oxygenated compounds—in the secondary products is more significant with glassy carbon than with graphite.

5 Conclusion

The electrochemistry of 4-methylanisole oxidation in methanol solutions has been investigated by linear voltammetry and preparative conversion in a batch cell. Potassium fluoride offers the best selectivity for the production of acetal, whereas use of perchlorate salts favours further oxidation of acetal to secondary products. The nature of the electrode material largely affects the electrode kinetics. Graphite and ''cut'' glassy carbon allow faster oxidation of anisole to acetal, with overall Tafel slopes near 70 mV/decade, in perfect agreement with previous observations [3]. In contrast, the surface treatment employed for preparation of commercial glassy carbon plates resulted in significant deactivation of the electrode surface resulting in two-fold increase in Tafel slope. An empirical kinetic model representing intermediate formation of ether as well as acetal oxidation was proposed to quantify the results of the batch tests.

The values of the fitted kinetic parameters obtained in the present study will be used in future work for quantitative analysis of the performance of new designs for electrochemical reactors for the production of anisaldehyde.

Acknowledgements Financial support for this work has been provided by the European Project Impulse (project reference ID NMP2-CT-2005–011816 of the 6th Framework Programme for Research and Technological Development of the European Union). The authors also wish to thank the French Ministry of Research for the PhD grant allocated to A.Attour. The mass spectroscopy analysis of selected samples was kindly carried out by Dr. A.Ziogas, Institut für Microtechnik, Mainz, Germany.

References

1. Venkatachalapathy MS, Ramaswami R, Udupa HVK (1958) Bull Acad Polon Sci Ser Sci Chim 6:478
2. Wendt H, Schneider H (1986) J Appl Electrochem 16:134
3. Wendt H, Bitterlich S (1992) Electrochim Acta 37:1951
4. Wendt H, Bitterlich S, Lodowicks E, Liu Z (1992) Electrochim Acta 37:1959
5. Kramer K, Robertson PM, Ibl N (1980) J Appl Electrochem 10:29
6. Lund H, Hammerich O (2001) Organic electrochemistry, 4th edn. Marcel Dekker, New York, p 1286
7. Lindermeir A, Horst C, Hoffmann U (2003) Ultrasonics Sonochem 10:223
8. Haj Said A, Mhalla FM, Amatore C, Verpeaux JN (1999) J Anal Chem 464:85
9. Sim BA, Milne PH, Griller D, Wagner DDM (1990) J Am Chem Soc 112:6635
10. Wendt H, Kreysa G (1999) Electrochemical engineering: science and technology in chemical and other industries. Springer-Verlag, Berlin, p 142
11. Ziogas A, Löwe H, Küpper M, Ehrfeld W (2000) Electrochemical microreactors: a new approch for microreaction technology, in microreaction technology: industrial prospects, IMRET3: Proceedings of the 3rd International Conference on Microreaction Technology, Frankfurt/Main. In: Ehrfeld W (ed). Springer-Verlag, Berlin, pp 136
12. Küpper M, Hessel V, Löwe H, Stark W, Jinkel J, Michel M, Schmidt-Traub H (2003) Electrochim Acta 48:2889
13. Rode S, Altmeyer S, Matlosz M (2004) J Appl Electrochem 34:671
14. Degner D, Barl M, Siegl HV (1980) Substituted benzaldehyde-dialkylacetal, US Patent 4284825. BASF Aktiengesellschaft, Germany
15. Degner D (1988) In: Steckhan E (ed) Topics in current chemistry, vol 148. Springer-Verlag, Berlin, pp 10–21
16. Bard AJ, Faulkner LR (1980) Electrochemical methods. John Wiley & Sons, New York, p 291
17. Tyn MT, Calus WF (1975) J Chem Eng Data 20:106
18. Siddiqi MA, Lucas M (1986) Can J Chem Eng 64:839